Micromagnetic simulation of ferromagnetic metamaterials with wire inclusions

Maria D. Amel'chenko⬡ and Sergei V. Grishin⬡[*]
Saratov State University, Saratov 410012, Russia

Feodor Yu. Ogrin
Department of Physics, University of Exeter, Exeter EX4 4QL, United Kingdom
and MaxLLG Ltd., Exeter Science Park, Exeter EX5 2FN, United Kingdom

Sergei A. Nikitov
Kotelnikov Institute of Radioengineering and Electronics of Russian Academy of Science, Moscow 125009, Russia

Left-handed (LH) metamaterials are generally structured materials possessing abnormal electromagnetic properties due to both negative permittivity and permeability. One of these properties is a backward wave (BW) propagation, in which the phase and group velocities are opposite to each other. Here we investigate the electrodynamic (dispersion and energy) characteristics of the BW existing in a magnetic LH metamaterial that is controlled by the external uniform magnetic field. Such a metamaterial is a host made from a μ-negative (ferromagnetic) nonconductive medium that contains a two-dimensional periodic structure of thin and isolated wires placed in the bias field directed either transversely or longitudinally to the electromagnetic wave propagation. A finite-difference time-domain–Landau-Lifshits-Gilbert (LLG) electromagnetic solver MaxLLG is used for the BW numerical simulations. This solver is based on the simultaneous usage of the Maxwell and LLG equations. By operating this software, the authors validate the existence of the BWs in the investigated LH metamaterial for two bias field orientations for various values of magnetic LH layer thickness and wire conductivity as well as for two connection types of wires with metallic planes that are placed on both sides of the metamaterial layer.

I. INTRODUCTION

Metamaterials are artificial structures, composed of periodic subwavelength-scale arrays with $T \ll \lambda$ (where T is an array period and λ is a wavelength). Metamaterials possess such electromagnetic properties that natural materials do not have. This electromagnetic behavior results from specific configurations and generally structured materials, composed of ordered elements. Apparently, one of the first metamaterial that was theoretically predicted [1,2] and experimentally studied [3,4] is a left-handed material (LHM). The first suggested LHM structure consists of an array of continuous conducting wires and nonmagnetic split-ring resonators (SRRs) [3]. The wire array exhibits plasmonic features that can be described with an effective permittivity ε_{eff}, while the SSR array behaves as an environment having an effective magnetic permeability μ_{eff}. These effective parameters are of resonant nature and both take negative values in a frequency band defined by both the element dimensions and lattice spacing. Therefore, LHMs are often referred to as double-negative metamaterials (DNMs) supporting backward wave propagation, in which the phase and group velocities are opposite to each other.

Starting from the 2000s, a number of studies devoted to magnetotunable LHMs have been presented [5–11]. Most

were based on the usage of either ferromagnets (FMs) or antiferromagnets (AFMs): natural materials possessing negative μ (μ-negative materials) either in the microwave (FMs) or terahertz (AFMs) ranges [12]. The combination of their properties with the properties of ε-negative materials, which are periodic arrays of thin wires, made it possible to realize DNMs without the use of additional subwavelength elements in the form of SRRs. Besides, the properties of such metamaterials could also be controlled with an external bias field. For the microwave range, FMs were used either in the form of films [6,8] and plates [9] of yttrium iron garnet or in the form of ferrite rods [10] or films of BaM type ferrites/hexaferrites [11]. Ferrite films LuBiIG [13] and AFM [14] were used for the terahertz range.

Dewar developed an analytical electrodynamic model of a FM LHM composed of long, thin, cladded metal wires within a nonconductive FM host [7]. In this model, a bias field is applied parallel to the wires and transversely to TE electromagnetic wave (EMW) propagation. He proposed a relation for the effective permittivity ε_{eff}, which includes the effective permeability μ_{eff} of the nonconductive FM host. It was shown that both effective material parameters of medium could have simultaneously negative values in a certain frequency range between two characteristic frequencies. One of them (higher frequency) was the antiresonance frequency f_{ar} and the other (lower frequency) was the plasma frequency f_p. In this frequency range, a backward EMW (BEMW) was predicted to

————————
[*]sergrsh@yandex.ru

be found. However, no experiments and numerical simulations that would confirm or deny Dewar's theory have been carried out.

Dewar's model was formulated for the infinite transversely magnetized FM metamaterial, because only here there is a single electrical component directed along the wires. It is well known [12] that for the longitudinal magnetization, when the bias field and the wave vector are codirected, an infinite FM supports quasitransverse electromagnetic (TEM) wave propagation. The TEM wave has two electrical components: One of them is directed along the wires and the other is directed perpendicularly to the wires. Such electrical field configuration will not support the double-negative properties of the FM metamaterial. However, if the longitudinally magnetized FM medium is limited in one direction (it has thickness), then the backward volume TE waves can exist. Their frequency band is then found between the ferromagnetic resonance frequency for longitudinal magnetization $f_{||}$ and the ferromagnetic resonance frequency for transverse magnetization $f_\perp$. In this band, the longitudinally magnetized FM layer has the properties of the μ-negative medium. To study the dispersion characteristics of these waves, the magnetostatic approximation is usually used. It is valid for thin FM films only [12]. In the work by Amel'chenko *et al.* [15], an approximate model of a longitudinally magnetized film of FM metamaterial with metal inclusions was presented. This model is based on both the dispersion equation (DE) for the longitudinally magnetized nonconductive FM layer and the relation for the effective permittivity ε_{eff}, describing the plasmonic properties of the wire array surrounded by an infinite isolation (vacuum) space by the use of the Drude theory. For such magnetized thin-film FM metamaterial, the backward volume TE waves exist in all frequency ranges, where both effective material parameters of the medium are negative. This band is found between the frequency $f_{||}$ and the antiresonance frequency f_{ar}. However, the confirmation of the backward volume TE wave existence in the frequency interval $f_{||} < f < f_{\text{ar}}$ was confirmed neither in experimental nor in numerical works.

Here we demonstrate the results of numerical simulation of the BEMW existing in the FM LHM with wire inclusions. For the numerical simulation, we use a three-dimensional (3D) finite-difference time-domain–Landau-Lifshits-Gilbert (FDTD-LLG) electromagnetic solver, MaxLLG [16]. The unique nature of this code is in the fact that it uses the LLG equation, which is solved in parallel with the Maxwell equations, providing the necessary material relations for permeability both statically and dynamically. This is of particular significance for the problems (such as in the case of this work) when the solutions are thought for magnetic materials combining metals, or in close proximity to them. Using standard magnetostatic solvers (OOMMF and MuMax) it is not possible to obtain the correct solution as those cannot account for electric fields. Equally, any standard commercial electromagnetic software (e.g., CST and HFSS), even though it allows some flexibility on providing the dynamic permeability, cannot offer an exact solution including demagnetizing effects associated with the geometry and the intrinsic properties of the material. Moreover, the LLG formulation in MaxLLG is solved exactly (without linearization), thus offering the results even for highly nonlinear applications. Using this software,
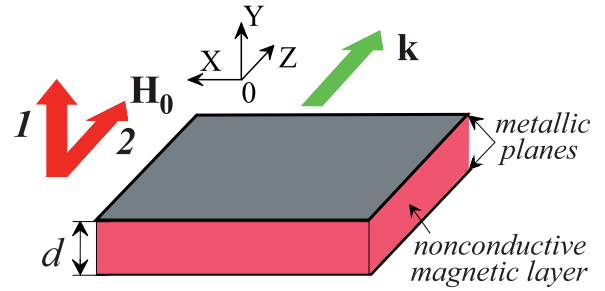

FIG. 1. A scheme of the homogeneous nonconductive FM layer that is metallized on both sides. The FM layer with suturation magnetization of $M_0 = 0.014$ T and dielectric constant of $\varepsilon = 16$ is placed in the uniform external magnetic field with two types of orientation. Orientation 1 corresponds to the normal type of magnetization and orientation 2 corresponds to the longitudinal type of magnetization.

here we show that the BEMW can be realized for both types of bias field orientation for various values of FM LHM layer thickness and wire conductivity as well.

II. ANALYTICAL MODELS AND CALCULATION RESULTS

A. The slow magnetic waves in a metallized ferromagnetic layer

The model of a homogeneous FM layer is based on a nonconductive FM layer of thickness d placed along the z axis between two parallel ideal conductive planes (see Fig. 1). A uniform external magnetic field $\mathbf{H}_0$ is applied parallel to the y axis and transversely to wave vector $\mathbf{k}$, which is aligned with the z axis ($\mathbf{H}_0||OY \perp \mathbf{k}||OZ$). By solving Maxwell's equations in the approximation of inhomogeneous plane EMWs, the following DE for normal magnetized FM can be obtained:

$$-k_y^2\left[k_y^2 + (1 + \mu)k^2 - 2\mu k_0^2\varepsilon\right]$$
$$= \mu k^4 - \left(\mu^2 + \mu - \mu_a^2\right)k^2 k_0^2\varepsilon + \left(\mu^2 - \mu_a^2\right)k_0^4\varepsilon^2, \quad (1)$$

where k_y is a quantized wave number in the y-axis direction (a transversal wave number), which can be expressed as

$$k_y = \frac{n\pi}{d}, \quad (2)$$

$n = \pm 1, 2, 3 \ldots$ is an index of volume EMW mode; k is a longitudinal wave number of the EMW propagating in FM in the z-axis direction; $k_0 = \omega/c$ is a wave number of EMW propagating in vacuum; $\omega = 2\pi f$ is a circular frequency; f is a liner frequency; c is a light velocity in free space; $\mu = (\omega_\perp^2 - \omega^2)/(\omega_{||} - \omega^2)$ and $\mu_a = (\omega_M\omega)/(\omega_{||} - \omega^2)$ are diagonal and off-diagonal components of the permeability tensor, respectively; $\omega_\perp = \sqrt{\omega_{||}\omega_{\text{ar}}}$ is a circular frequency of FM resonance for transverse magnetization; $\omega_{\text{ar}} = \omega_{||} + \omega_M$ is a circular frequency of FM antiresonance; $\omega_{||} = \gamma H_0$ is a circular frequency of FM resonance for longitudinal magnetization $\omega_M = 4\pi\gamma M_0$; $\gamma/(2\pi) = 2.8$ MHz/Oe is a gyromagnetic ratio; and $4\pi M_0$ is saturation magnetization.

For an infinite transversely magnetized FM medium ($d \to \infty$ and $k_y = 0$), Eq. (1) can be rewritten as two DEs [12]. One of them corresponds to the transverse electric (TE) wave

$$k^2 - k_0^2\mu_{\text{eff}\perp 1}\varepsilon = 0, \quad (3)$$

possessing three components of electromagnetic field e_y, h_x, h_z that are not equal to zero and the other DE corresponds to the transverse magnetic (TM) wave,

$$k^2 - k_0^2 \mu_{\text{eff}\perp 2} \varepsilon = 0, \tag{4}$$

where $\mu_{\text{eff}\perp 1}$ is the effective permeability of medium supporting TE wave propagation,

$$\mu_{\text{eff}\perp 1} = \frac{\mu^2 - \mu_a^2}{\mu}, \tag{5}$$

and $\mu_{\text{eff}\perp 2}$ is the effective permeability of medium supporting TM wave propagation and is equal to 1.

In the magnetostatic approximation, when $k \gg k_0$, the DE (1) is transformed to the DE for slow forward volume magnetostatic waves (FVMSWs),

$$k_y^2 + \mu k^2 = 0. \tag{6}$$

The FVMSWs existing in the metallized FM film are the TE waves possessing three components of the electromagnetic field:

$$e_{0x} = \frac{k_0}{k} A \sin(k_y y),$$
$$h_{0y} = A \sin(k_y y),$$
$$h_{0z} = j \frac{k}{k_y} A \cos(k_y y), \tag{7}$$

where A is an arbitrary constant. However, in contrast to the TE waves existing in the transversely magnetized infinite FM medium, the FVMSWs do not have the e_y component of the electric field directed along the wires.

For the longitudinally magnetized FM layer ($\mathbf{H}_0 || \mathbf{k} || OZ$), covered by two ideally conductive planes, the DE has the following form:

$$-k_y^2 \left[\mu k_y^2 + (1 + \mu) k^2 - \left(\mu^2 + \mu - \mu_a^2 \right) k_0^2 \varepsilon \right]$$
$$= k^4 - 2\mu k^2 k_0^2 \varepsilon + \left(\mu^2 - \mu_a^2 \right) k_0^4 \varepsilon^2, \tag{8}$$

where k_y is obtained as [17]

$$a_1 b_2 \sin(\alpha_1) \cos(\alpha_2) - a_2 b_1 \sin(\alpha_2) \cos(\alpha_1) = 0,$$
$$a_1 b_2 \sin(\alpha_2) \cos(\alpha_1) - a_2 b_1 \sin(\alpha_1) \cos(\alpha_2) = 0, \tag{9}$$

where $\alpha_1 = k_{y1} d/2$, $\alpha_2 = k_{y2} d/2$, $k_{y3} = -k_{y1}$, $k_{y4} = -k_{y2}$, $a_1 = b_1 = 1$, $a_2 = -k_{y1}(\mu k_{y1}^2 + k^2 - \mu k_0^2 \varepsilon)/(\mu_a k k_0^2 \varepsilon)$, and $b_2 = -k_{y2}(\mu k_{y2}^2 + k^2 - \mu k_0^2 \varepsilon)/(\mu_a k k_0^2 \varepsilon)$.

Equation (9) can be written as

$$k_{y1,2} = \pm \left(\frac{n\pi}{d} \right) + \sqrt{\frac{-\left[\mu \left(\frac{n\pi}{d} \right)^2 + k^2 - \mu k_0^2 \varepsilon \right]}{3\mu}}. \tag{10}$$

If we set $k_y = 0$, then the DE (8) is transformed into two DEs whose solutions correspond to the quasi-TEM waves possessing four transversal components of the electromagnetic field e_x, e_y, h_x, h_y that are not equal to zero [12]:

$$k^2 - k_0^2 \mu_{\text{eff}||1} \varepsilon = 0, \tag{11a}$$

$$k^2 - k_0^2 \mu_{\text{eff}||2} \varepsilon = 0, \tag{11b}$$

where

$$\mu_{\text{eff}||1} = \mu + \mu_a, \tag{12a}$$

$$\mu_{\text{eff}||2} = \mu - \mu_a. \tag{12b}$$

In the magnetostatic approximation, the DE (8) is transformed into the DE for slow backward volume magnetostatic waves (BVMSWs),

$$\mu k_y^2 + k^2 = 0. \tag{13}$$

The BVMSWs like the FVMSWs are also the TE waves possessing three components of the electromagnetic field in thin films ($k_y \gg k_0$):

$$e_{0x} = -\frac{k k_0}{k_y^2} B \sin(k_y y),$$
$$h_{0y} = B \sin(k_y y),$$
$$h_{0z} = j \frac{k}{k_y} B \cos(k_y y), \tag{14}$$

where B is an arbitrary constant. The BVMSWs also do not have the e_y component of the electric field directed along the wires. In the magnetostatic approximation, the Eq. (10) is transformed into the Eq. (2).

To determine that a MSW is a purely magnetic wave, its electric and magnetic energies are calculated. The averaged energy W of the electromagnetic field existing in an anisotropic lossless dispersive medium is calculated as [18]

$$W = W_e + W_h, \tag{15}$$

where the averaged energy of the electric field W_e is

$$W_e = \frac{1}{16\pi V} \int_V \text{Re} \left\langle \mathbf{e} \left\{ \frac{\partial(\omega \bar{\varepsilon}^*)}{\partial \omega} \mathbf{e}^* \right\} \right\rangle dV, \tag{16a}$$

and the averaged energy of the magnetic field W_h is

$$W_h = \frac{1}{16\pi V} \int_V \text{Re} \left\langle \mathbf{h} \left\{ \frac{\partial(\omega \bar{\mu}^*)}{\partial \omega} \mathbf{h}^* \right\} \right\rangle dV, \tag{16b}$$

V is the volume of the anisotropic dispersive medium, $\mathbf{e}$ and $\mathbf{h}$ are the alternating electric and magnetic fields, the sign $*$ denotes the complex conjugate, and $\bar{\varepsilon}$ and $\bar{\mu}$ are the tensors of the permittivity and permeability. The permittivity of the homogeneous FM medium is scalar, while the permittivity of the FM metamaterial is frequency dependent. When $\mathbf{H}_0 || OY$, the permeability tensor has the following form:

$$\bar{\mu} = \begin{pmatrix} \mu & 0 & -j\mu_a \\ 0 & 1 & 0 \\ j\mu_a & 0 & \mu \end{pmatrix}, \tag{17a}$$

and if $\mathbf{H}_0 || OZ$, then its form is

$$\bar{\mu} = \begin{pmatrix} \mu & j\mu_a & 0 \\ -j\mu_a & \mu & 0 \\ 0 & 0 & 1 \end{pmatrix}. \tag{17b}$$

The energy characteristics also include a group velocity $\mathbf{V}_g$ and a velocity of energy flow $\mathbf{V}_p$ that are calculated on the base of following expressions:

$$\mathbf{V}_g = \partial \omega / \partial \mathbf{k}, \tag{18}$$

$$\mathbf{V}_p = \mathbf{P}/W, \tag{19}$$

where

$$\mathbf{P} = \frac{c}{8\pi V} \int_V \text{Re}(\mathbf{e} \times \mathbf{h}^*) dV. \tag{20}$$
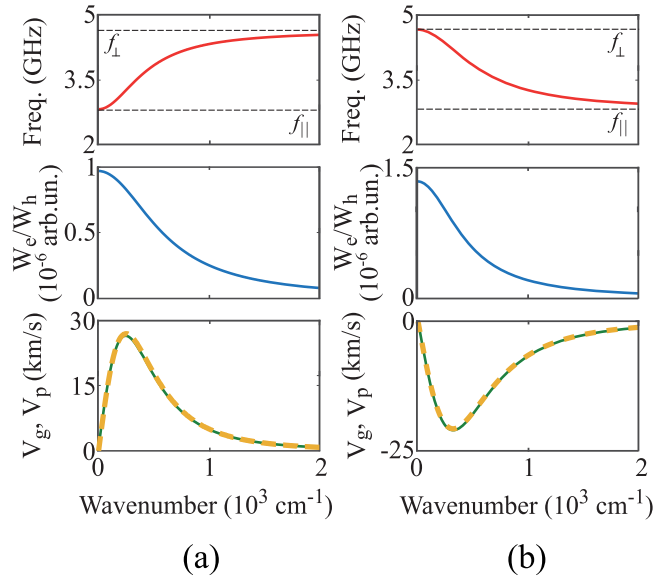
FIG. 2. The electrodynamic characteristics of slow FVMSW (a) and BVMSW (b) existing in normally (a) and longitudinally (b) magnetized FM thin films that are metallized on both sides. In the upper panels of (a) and (b) there are the dispersion characteristics of both volume MSWs (red solid lines), in the middle panels of (a) and (b) there are the ratio of electric and magnetic energies of these waves (blue solid lines), and in the bottom panels of (a) and (b) there are their group (green solid lines) and energy flow (yellow dashed lines) velocities. The calculations were made for $H_0 = 795.8$ A/m, $M_0 = 0.014$ T, $d = 10$ μm, and $n = 1$.

Figure 2 demonstrates the electrodynamic (dispersion and energy) characteristics of the slow FVMSW and BVMSW calculated on the basis of Eqs. (2), (6), (13)–(20). It can be seen that the FVMSW existing in a normally magnetized FM film has normal positive dispersion and the BVMSW existing in a longitudinally magnetized FM film has abnormal negative dispersion [see upper fragments in Figs. 2(a) and 2(b)]. Both types of MSWs are located in the same frequency range, where $\mu < 0$ and $\varepsilon > 0$. The magnetic energy of both MSW types significantly prevails over the electric energy throughout the whole k range [see middle fragments in Figs. 2(a) and 2(b)]; therefore the MSWs are the purely magnetic waves. Curves of group and energy flow velocities coincide for both MSW types [see bottom fragments in Figs. 2(a) and 2(b)]. For the FVMSW, both velocities are positive and they coincide with the phase velocity direction. For the BVMSW, these velocities are negative and they are opposite to the phase velocity direction.

B. The slow electromagnetic waves in a metallized ferromagnetic metamaterial layer

A model of infinite FM metamaterial was developed by Dewar for a nonconductive transversely magnetized FM host containing a square two-dimensional array of thin conductive round wires cladded with a nonmagnetic dielectric layer [7]. The bias field $\mathbf{H}_0$ is applied along the wires. Assuming that the media has effective properties, the lattice constant T is supposed to be much smaller than the wavelength of the TE
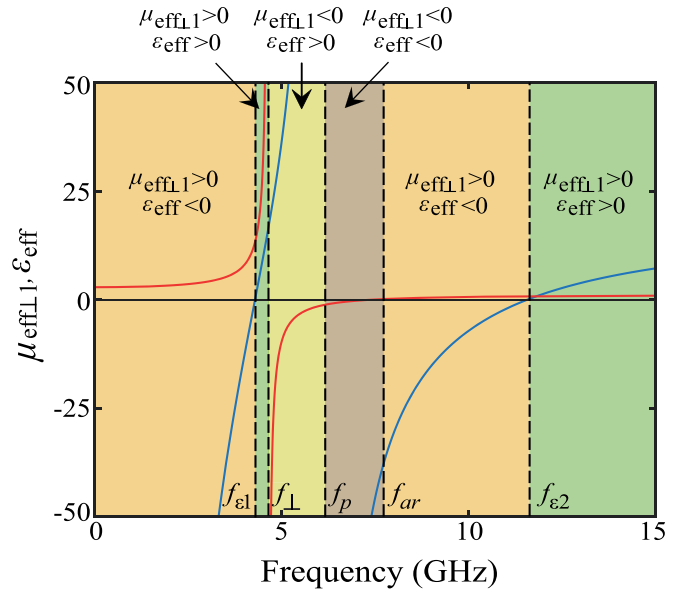

FIG. 3. The frequency dependencies of the effective permeability $\mu_{\mathrm{eff}\perp 1}$ (red solid lines) and the effective permittivity $\varepsilon_{\mathrm{eff}}$ (blue solid lines) calculated for the transversely magnetized infinite FM metamaterial. Calculations were made for $H_0 = 795.8$ A/m, $M_0 = 0.014$ T, $\varepsilon_r = 16$, $r_1 = 100$ μm, $r_2 = 300$ μm, and $T = 2$ mm.

wave propagating normally to the wires. The TE wave has one component of the electric field directed along the wires and ensuring the polarization of charges in this direction. The isolating layer surrounding the wires is necessary for protection of their plasmonic features from the ferromagnetic resonance, as magnetic moments of the host changing their directions can ruin electron order. The wire radius r_1, the outer radius of the cladding material r_2, and the lattice constant T were chosen such that $r_2 \cong \sqrt{r_1 T}$ and $r_1 \ll r_2 \ll T$. Dewar has derived expressions for the effective dielectric function $\varepsilon_{\mathrm{eff}}$ and the plasma frequency ω_p that include $\mu_{\mathrm{eff}\perp 1}$ of the host [7]:

$$\varepsilon_{\mathrm{eff}} = \varepsilon_r \left\{ 1 - \frac{\omega_p^2}{\omega^2 + i\alpha} \right\}, \qquad (21)$$

$$\omega_p^2 \cong \frac{2\pi}{\varepsilon_f T^2 \mu_0 \left[\ln \frac{r_2}{r_1} + \mu_{\mathrm{eff}\perp 1} \left(\ln \frac{T}{r_2} - \frac{3 + \ln 2 - \pi/2}{2} \right) \right]}, \qquad (22)$$

where $\alpha = \varepsilon_f \omega \omega_p^2 / \sigma_{\mathrm{eff}}$, $\varepsilon_f = \varepsilon_0 \varepsilon_r$ is the absolute permittivity of the FM, $\varepsilon_0 = 1/(\mu_0 c^2)$ is the vacuum constant, μ_0 is the vacuum permeability, ε_r is the relative permittivity of the FM, $\sigma_{\mathrm{eff}} = \pi r_1^2 \sigma / T^2$ is the effective conductivity of the wire array, and σ is the conductivity of the wires. Hereafter, we consider a structure that lacks of losses ($\alpha = 0$). Equation (22) was obtained by assuming that the current density is uniform throughout the wire, e.g., the wire radius is much smaller than the skin depth δ: $r_1 \ll \delta = \sqrt{2/\mu_0 \sigma \omega}$.

Figure 3 demonstrates the frequency dependencies of the effective material parameters of the transversely magnetized FM metamaterial that are calculated using the Eqs. (5), (21), and (22). In contrast to the homogeneous FM, the effective permittivity of the FM metamaterial has negative values in two frequency ranges. One of them starts from the low

frequencies and extends to a frequency $f_{\varepsilon 1}$, at which the effective permittivity passes through zero. This frequency is lower than the FM resonance frequency $f_\perp$, so at the frequencies $f < f_{\varepsilon 1}$ the effective permeability $\mu_{\mathrm{eff}\perp 1}$ has positive values and the effective permittivity has negative values ($\mu_{\mathrm{eff}\perp 1} > 0$ and $\varepsilon_{\mathrm{eff}} < 0$). The other frequency range starts from the plasma frequency f_p, at which it passes through a resonance and extends to a frequency $f_{\varepsilon 2}$, where it passes through zero. The plasma frequency f_p lies between the FM resonance $f_\perp$ and the FM antiresonance f_{ar} frequencies, while the frequency $f_{\varepsilon 2}$ is higher than the FM antiresonance frequency f_{ar}. At the last frequency, the effective permeability $\mu_{\mathrm{eff}\perp 1}$ passes through zero. Thus, the effective permeability has positive values and the effective permittivity has negative values ($\mu_{\mathrm{eff}\perp 1} > 0$ and $\varepsilon_{\mathrm{eff}} < 0$) in the frequency interval $f_{\mathrm{ar}} < f < f_{\varepsilon 2}$. In the frequency interval $f_p < f < f_{\mathrm{ar}}$, the effective permittivity and permeability have negative values simultaneously ($\mu_{\mathrm{eff}\perp 1} < 0$ and $\varepsilon_{\mathrm{eff}} < 0$).

Besides, the effective permittivity and permeability $\mu_{\mathrm{eff}\perp 1}$ have positive values simultaneously ($\mu_{\mathrm{eff}\perp 1} > 0$ and $\varepsilon_{\mathrm{eff}} > 0$) in two frequency ranges. One of them is located between the frequencies $f_{\varepsilon 1}$ and $f_\perp$. The other starts from the frequency $f_{\varepsilon 2}$ and extends to the higher-frequency region. The obtained results indicates that such metamaterial will support the EMW propagation only in three frequency intervals: $f_{\varepsilon 1} < f < f_\perp$, $f_{\varepsilon 2} < f$, and $f_p < f < f_{\mathrm{ar}}$. In the last case, the FM metamaterial possesses the properties of DNM supporting the backward wave propagation.

In the Dewar's model, a plane EMW has one electric field component that is directed along the wires. Such situation is realized only for the transversely magnetized infinite FM medium. For other cases associated both with a change in the direction of the bias field and with the usage of boundary conditions in the form of semi-infinite free space on both sides of the FM medium, the EMW will have the nonzero transverse components of the electric field. These electric components will transversely polarize the charges on the side walls of the wires and destroy the charge polarization along the wires. As a result, the double-negative properties of the FM metamaterial will disappear. To solve this problem, we propose to use the boundary conditions in the form of ideally conductive metallic planes connected to the wire array. This form connection of the metallic planes with the wires will create the closed electric circuits in that the electric field component directed along the wires will support the flow of electric current along the wires. We believe that these boundary conditions, applied to the magnetized FM metamaterial layer, will return the properties of a doubly negative medium to the mentioned above layer.

To construct an approximate model of a normally magnetized FM metamaterial layer in contact with metallic planes on both sides, we will use the DE (1), describing the properties of a normally magnetized FM layer, and the expressions obtained for the transverse wave number (2), effective permittivity (21), and permeability (5). Figure 4 represents a scheme of the investigated structure. The model does not take into account the polarization of charges across the wires and is valid for relatively thick FM metamaterial layers in that the electric field component along the wires is greater than the electric field components across the wires. This statement
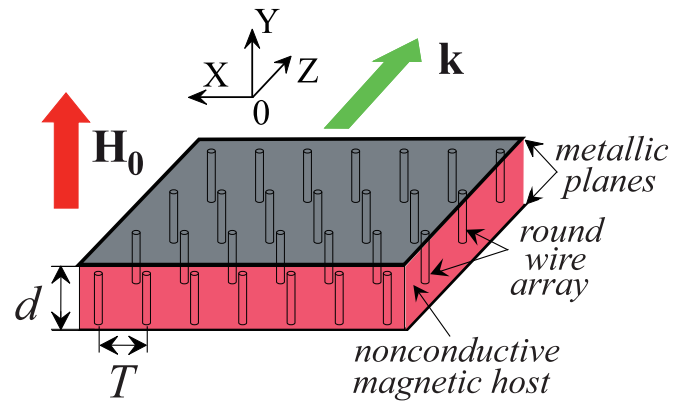

FIG. 4. A scheme of the normally magnetized FM metamaterial layer that is metallized on both sides. The metamaterial layer consists of the nonconductive FM host with suturation magnetization of $M_0 = 0.014$ T that contains 2D conductive wire array. The wires of the array are cladded with nonmagnetic dielectric layer.

will be subsequently confirmed by the results of numerical simulation.

In Fig. 5, the electrodynamic characteristics of the slow forward and backward waves existing in the normally magnetized FM metamaterial layer that is metallized on both sides are presented. It can be seen that forward wave with normal positive dispersion and backward wave with abnormal negative dispersion exist simultaneously in different
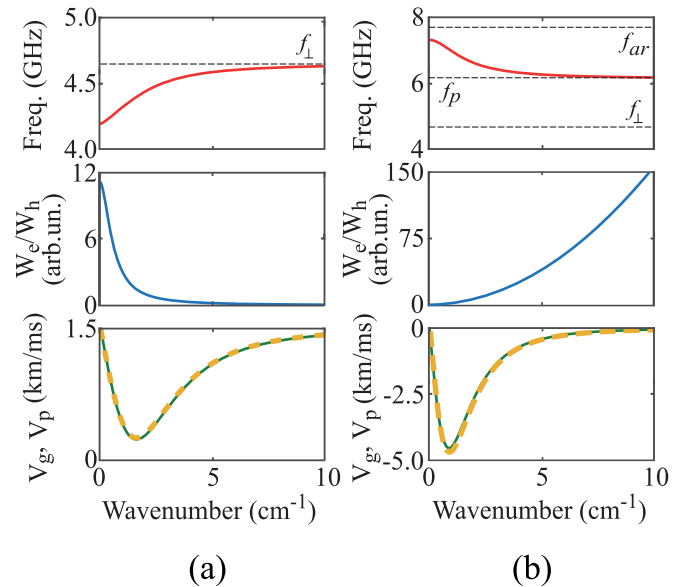

FIG. 5. The electrodynamic characteristics of slow FEMW (a) and BEMW (b) existing in normally magnetized FM metamaterial layer that is metallized on both sides. In the upper panels of (a) and (b) there are the dispersion characteristics of both slow waves (red solid lines), in the middle panels of (a) and (b) there are the ratio of electric and magnetic energies of these waves (blue solid lines), and in the bottom panels of (a) and (b) there are their group (green solid lines) and energy flow (yellow dashed lines) velocities. The calculations were made for $H_0 = 795.8$ A/m, $M_0 = 0.014$ T, $\varepsilon_r = 16$, $r_1 = 100$ μm, $r_2 = 300$ μm, $T = 2$ mm, $d = 1$ cm, and $n = 1$.

frequency ranges [see upper fragments in Figs. 5(a) and 5(b)]. The slow forward wave exists in the frequency interval $f_{\varepsilon 1} < f < f_\perp$, where $\mu_{\mathrm{eff}\perp 1} > 0$ and $\varepsilon_{\mathrm{eff}} > 0$ (see Fig. 3). In this frequency range, the volume MSWs exist in the homogeneous FM film (see Fig. 2). The slow backward wave exists in higher-frequency interval $f_p < f < f_{\mathrm{ar}}$, where the effective parameters of the FM metamaterial are double negative ($\mu_{\mathrm{eff}\perp 1} < 0$ and $\varepsilon_{\mathrm{eff}} < 0$; see Fig. 3). In this frequency range, the volume MSWs do not exist in the homogeneous FM film. As follows from the results presented in middle fragments in Figs. 5(a) and 5(b), both types of slow waves are the EMWs. As for the slow forward EMW (FEMW), the electric energy prevails over the magnetic energy, while k has small values, and the magnetic energy prevails over the electric energy near the FM resonance frequency $f_\perp$ at the large values of k ($k \to \infty$). For the BEMW, the situation is the opposite. Here the magnetic energy prevails over the electric energy, while the k has small values, and the electric energy prevails over the magnetic energy near the plasma frequency f_p at the large values of k ($k \to \infty$). Curves of group and energy flow velocities coincide for both EMWs [see bottom fragments in Figs. 5(a) and 5(b)]. Both velocities are positive for the slow FEMW and negative for the slow BEMW.

III. NUMERICAL MODELS AND CALCULATION RESULTS

A. Infinite ferromagnetic and ferromagnetic metamaterial with metal wire inclusions

The numerical simulation of the wave forms existing in the homogeneous FM and FM metamaterial with the wire inclusions (see Fig. 6) was carried out using MaxLLG software [16]. This code is based on the FDTD solution where the LLG equation of magnetization motion is solved in parallel with the Maxwell equations. Calculation of LLG uses a stable iterative algorithm that incorporates anisotropy and exchanged fields within the FDTD grid [19]. In such a way, the FDTD-LLG scheme provides simulation of the wide-band interaction of electromagnetic waves with magnetic structures. Further details of the simulation process are introduced in the Supplemental Material [20] (see also Refs. [7,19,21] therein).

Figures 7(a) and 7(c) demonstrate the results of two-dimensional Fourier transform of the space-time map obtained for the infinite FM medium (without the wire inclusions) that is placed in both transversal [see Fig. 7(a)] and longitudinal [see Fig. 7(c)] bias fields. The presented numerical results (yellow dots) are compared with the analytical ones (red lines) obtained using Eqs. (3), (5), (11a), (11b), (12a), and (12b). As can be seen in Fig. 7(a), the dispersion curves produced by the analytical model for the transversal bias field orientation have an excellent agreement with the simulation results. One of the waves is the fast TE wave that has a cutoff frequency equal to f_{ar}, whereas another is the slow TE wave that has only a limiting frequency equal to $f_\perp$. In Fig. 7(c), the results for the longitudinal bias field orientation are presented. Here the analytical dispersion curves of quasi-TEM waves existing in the longitudinally magnetized FM are compared with the dispersion curves obtained from the numerical simulation. It can be seen that three quasi-TEM
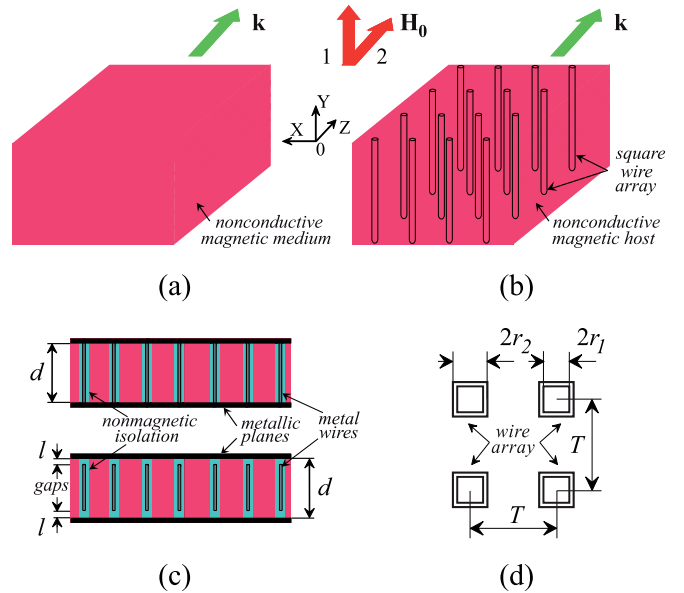

FIG. 6. The schematics of the infinite FM medium (a), the infinite FM metamaterial with square wire inclusions (b), and the FM metamaterial layer with various types of square wire connections to the metallic planes (c). In (d), the 2D wire array (a top view) consisting of the square wires with side $2r_1$ cladded with nonmagnetic square dielectric layer of side $2r_2$ is presented. In (a) and (b), orientation 1 of the bias field corresponds to the transverse type of magnetization and orientation 2 corresponds to the longitudinal type of magnetization.

waves with normal dispersion are obtained. Two of them are the fast waves and one is the slow wave. One of the fast quasi-TEM waves has the same cutoff frequency f_{ar} as the fast TE wave for the transverse bias field orientation does. Another fast quasi-TEM wave does not have the cutoff frequency. In contrast to the slow TE wave, the slow quasi-TEM wave has the lower limiting frequency that is $f_{||}$. Thus, for the longitudinal bias field orientation, we also have a good agreement between the results of the analytical theory and the numerical simulation.

At the next step, we considered the FM metamaterial consisting of the periodic array of metal wires incorporated in the FM host. The conductivity of the wires was chosen to be approximately equal to the conductivity of silver. The dispersion curves of the EMWs obtained using MaxLLG software for the infinite FM metamaterial placed in the bias field directed along or perpendicularly to the metal wires are presented in Fig. 7(b) and Fig. 7(d), respectively. In Fig. 7(b), the numerical results are compared with the analytical calculations made using Eqs. (3), (5), (21), and (22). When the wire array is embedded into the transversely magnetized FM host [see Fig. 7(b)], the frequency band of the slow FEMW is narrowed due to it has a cutoff frequency that is practically equal to the frequency $f_{\varepsilon 1}$ calculated from the analytical theory [see an insert in Fig. 7(b)]. The cutoff frequency of the fast EMW is shifted toward higher frequencies and is equal to the frequency $f_{\varepsilon 2}$ (see Fig. 3). In addition, the slow BEMW appears in the frequency range between the plasma frequency f_p (the limiting frequency) and the FM antiresonance frequency f_{ar}
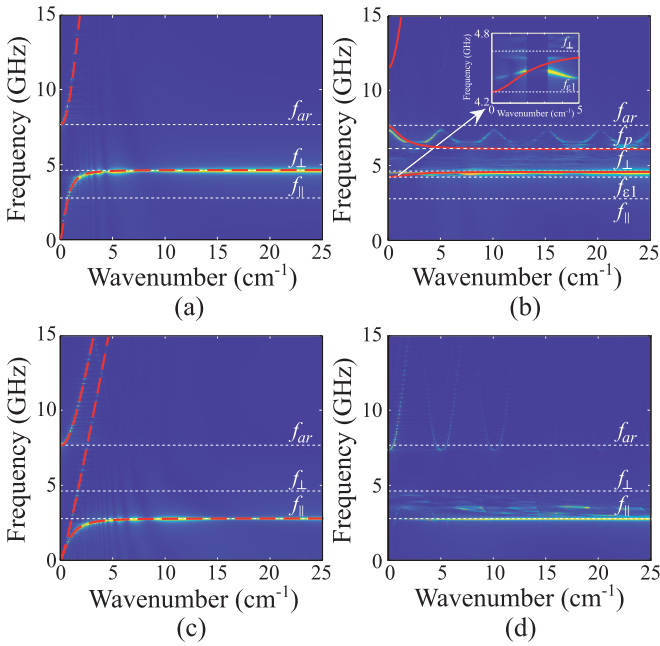
FIG. 7. The dispersion curves of TE [(a) and (b)] and quasi-TEM [(c) and (d)] EMWs existing in transversely [(a) and (b)] and longitudinally [(c) and (d)] magnetized infinite FM [(a) and (c)] and FM metamaterial [(b) and (d)]. The dispersion curves were simulated using the MaxLLG software (yellow lines), obtained on the base of Eqs. (3) and (11a) (dashed red lines) and calculated using the Dewar's analytical theory (solid red lines). In (b), the insert demonstrates an enlarged fragment of the FEMW dispersion curve in the range of small values of k. The calculations were made for $H_0 = 795.8$ A/m, $M_0 = 0.014$ T, $\varepsilon_r = 16$, $r_1 = 100$ μm, $r_2 = 300$ μm, $T = 2$ mm, and $\sigma = 10^8$ S/m.
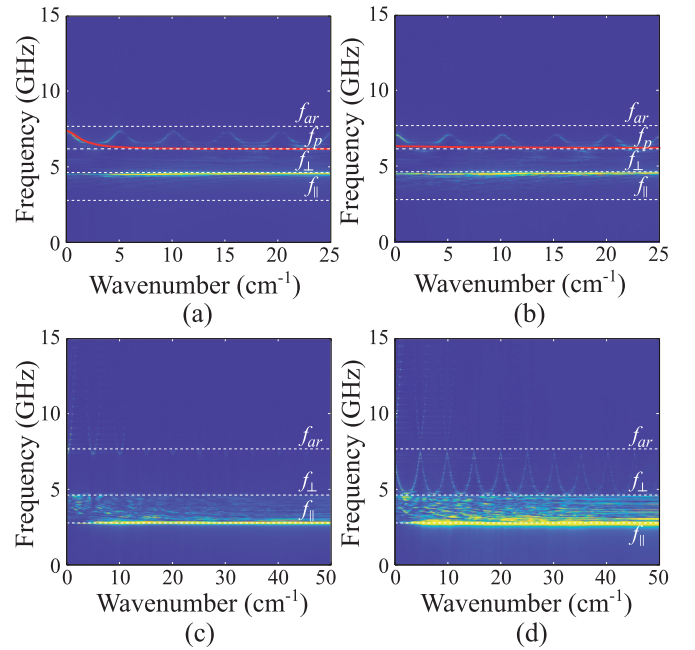
FIG. 8. The dispersion curves of EMWs existing in normally [(a) and (b)] and longitudinally [(c) and (d)] magnetized FM metamaterial layer. The curves were obtained for various values of thickness d: 1.1 cm [(a) and (c)], 1.5 mm (b), and 5 mm (d). The EMW dispersion curves were simulated using the MaxLLG software (yellow lines) and obtained from the approximate analytical theory (red lines). The calculations were made for $H_0 = 795.8$ A/m, $M_0 = 0.014$ T, $\varepsilon_r = 16$, $r_1 = 100$ μm, $r_2 = 300$ μm, $T = 2$ mm, and $\sigma = 10^8$ S/m.

B. A layer of ferromagnetic metamaterial with metal or semiconductor wire inclusions placed inside a parallel plate waveguide

Here we demonstrate the results of numerical simulation of the spectrum of EMWs existing in a FM metamaterial layer for two bias field orientations. The FM metamaterial layer is placed between two ideally conductive metallic planes. Such structure configuration corresponds to a microstrip waveguide filled with FM metamaterial. From the analytical model suggested for the normally magnetized FM metamaterial layer, it follows that all three electric components of the electromagnetic field are nonzero in thick layers. In contrast to this, in thin films only one electric component exists and it is transversely oriented to the wires [see Eq. (7)]. Analog situation is observed for the longitudinally magnetized FM metamaterial layer [see Eq. (14)]. Further, we will show that the contact of conductive wires with metallic planes provides the presence of the BEMW in both thick and thin normally magnetized FM metamaterial layers. In longitudinally magnetized FM metamaterial layers, the BEMW will be observed only in relatively thin layers.

The simulated dispersion curves of EMWs existing in the normally magnetized FM metamaterial layer with various values of thickness are shown in Figs. 8(a) and 8(b). It can be seen that the BEMW is observed both in thick [see Fig. 8(a)] and in relatively thin [see Fig. 8(b)] FM metamaterial layers. In both cases, the electric field component directed along the

(the cutoff frequency), where effective material parameters have negative values simultaneously (see Fig. 3). The discrepancy between the analytical and numerical results does not exceed 4% at the cutoff frequencies. Besides, the dispersion characteristic of the backward wave obtained by the use of numerical simulation contains the recurring regions due to the wave scattering from the periodic structure. This statement can be confirmed by the calculation of the first Bragg resonance wave number ($k_{B1} = \pi m/T$, where $m = 1$) that has a value $k_{B1}/(2\pi) = 2.5$ cm^{-1}. It is seen that the dispersion curve of the backward wave obtained from the analytical theory lacks these resonances due to the effective medium approximation.

According to the results shown in Fig. 7(d), the backward wave is not observed, when the bias field is codirected with the wave vector of the quasi-TEM EMW. In this case, the polarization of charges along the wires is disrupted due to the polarization of charges across the wires, induced by the transverse component of the electric field. Moreover, the upper branch of the fast quasi-TEM EMW is shifted to the lower frequencies and its cutoff frequency lies just under the frequency of f_{ar}. Thus, the numerical simulation goes to prove that the backward wave exists only in the transversely magnetized infinite FM metamaterial.

wires (e_y) is large enough to allow current to flow along the wires.

Comparing the dispersion curves of EMWs existing in the infinite and limited FM metamaterials, it is clear that the cutoff frequency of the fast EMW shifts to higher frequencies, beyond the considered range, and the cutoff frequency of the slow BEMW shifts to lower frequencies and tends to its limiting frequency with a decrease of the layer thickness. We also compared the results of numerical simulations with the results, obtained within the framework of the approximate analytical theory, and established the limit of its applicability. The approximate analytical theory results demonstrate a good agreement with the numerical simulation ones only for relatively thick normally magnetized FM metamaterial layers of $d > 1$ cm [see Fig. 8(a)]. For thinner FM metamaterial layers, the discrepancy is increased [see Fig. 8(b)], because one of the electric components (e_x) directed transversely to the wires is increased [see Eq. (7)].

However, the most intriguing results are shown in Figs. 8(c) and 8(d) for a strip waveguide filled with the longitudinally magnetized FM metamaterial layer. As analytic theory suggested, the BEMW does not exist in the longitudinally magnetized infinite FM metamaterial [see Fig. 7(d)]. As shown in Fig. 8(c), the similar situation is observed also in the relatively thick FM metamaterial layers, when $d > 1$ cm. In this case, only multimode spectrum of slow volume EMWs exists in the frequency interval of $f_{||} < f < f_\perp$. However, if a layer thickness satisfies approximately the following conditions: $d/2 \cong T = \lambda_{B1}/2$ (where λ_{B1} is a wavelength corresponding to the first Bragg resonance), then the BEMW appears in the frequency interval of $f_\perp < f < f_{ar}$, where $\mu_{\text{eff}||1} < 0$. The dispersion curve of the BEMW also contains the recurring regions for the wave numbers satisfying the Bragg condition [see Fig. 8(d)] and occupies the whole frequency interval of $f_\perp < f < f_{ar}$. It indicates that the ε_{eff} is negative throughout this range in contrast to the normal magnetization case.

For both values of thickness of the longitudinally magnetized FM metamaterial layer, the electric field component e_y directed along the wires is much less than the electric field component e_x directed transversely to the wires. We suggest that the e_y component can create the effective electric current along the wires only when the electric field lines from the adjacent wires are closed on each other. Such situation will be realized when the condition $d/2 \cong T$ is met. As a result, the BEMW appears.

In Figs. 9(a) and 9(c), we demonstrate the presence of the BEMW even in thin FM metamaterial films, when only one electric field component, perpendicular to the wires, is predicted by the magnetostatic approximation for two bias field orientations [see Eqs. (7) and (14)]. It can be seen that the BEMW exists at both bias filed orientations in the same frequency range, where both effective material parameters of the FM metamaterial are negative. The dispersion curves of this wave are narrower for both magnetization cases compared to the ones existing in thicker FM metamaterial layers considered previously [see Figs. 8(b) and 8(d)]. However, the bandwidth of the BEMW is wider for the longitudinal magnetization case in comparison with the normal magnetization case. Besides the BEMW, the BVMSWs are also observed in
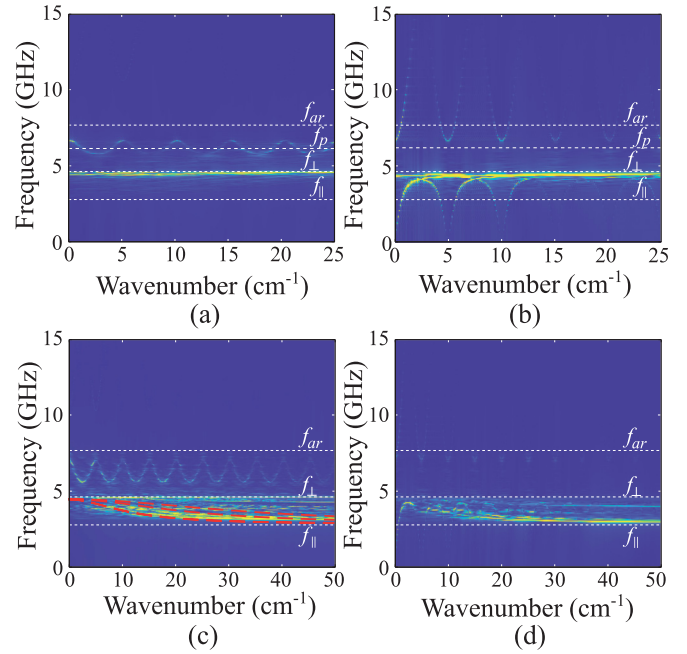

FIG. 9. The dispersion curves of EMWs existing in normally [(a) and (b)] and longitudinally [(c) and (d)] magnetized and metallized on both sides thin-film FM metamaterial. The curves were obtained for two types of wire connections with metallic planes. In (a) and (c), the wires are in a direct contact with the metallic planes. In (b) and (d), the wires are separated from the metallic planes by the gaps of a width $l = 100$ μm. The EMW dispersion curves were simulated using the MaxLLG sofware (yellow lines) and obtained in the magnetostatic approximation (dashed red lines). The calculations were made for $H_0 = 795.8$ A/m, $M_0 = 0.014$ T, $\varepsilon_r = 16$, $r_1 = 100$ μm, $r_2 = 300$ μm, $T = 2$ mm, $d = 0.5$ mm, and $\sigma = 10^8$ S/m.

the longitudinally magnetized thin-film FM metamaterial but in the frequency range of $f_{||} < f < f_\perp$ [see Fig. 9(c)], where $\mu_{\text{eff}||1} < 0$ and $\varepsilon_{\text{eff}} > 0$. The simulated dispersion curves of the first three volume modes of the BVMSWs correlate with the theoretical ones obtained in the magnetostatic approximation using the DE (8) [see red solid lines in Fig. 9(c)]. Thus, the spectrum of EMWs existing in the longitudinally magnetized thin-film FM metamaterial contains two types of the backward waves (BEMW and BVMSWs) located in different frequency ranges. For the normal bias filed orientation, there is only one type of the backward waves—the BEMW.

In Figs. 9(b) and 9(d), we also considered the case when the wires are not connected to metallic planes. Here, as predicted by the analytical theory, the BEMW does not exist in the FM metamaterial layers at the any types of bias field orientation.

As well as the wire connection with metallic plates, the wire's conductivity also affects plasmonic features. Here we consider the wires with two values of the conductivity (experimentally this can be achieved using the semiconductors). One of them corresponds to carbon (graphite) [see Figs. 10(a) and 10(c)], and the other corresponds to germanium [see Figs. 10(b) and 10(d)]. From the numerical simulation, it follows that the BEMW exists for both types of bias field
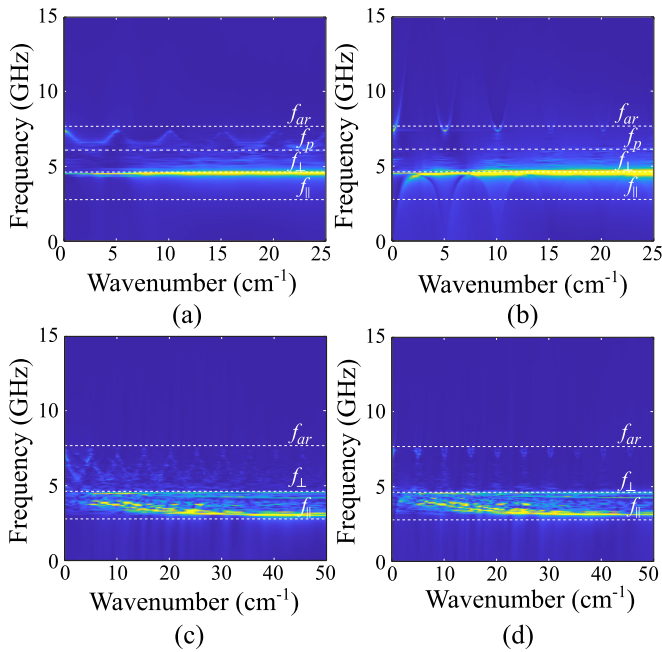
FIG. 10. The dispersion curves of EMWs calculated for normally [(a) and (b)] and longitudinally [(c) and (d)] magnetized thin-film FM metamaterial with semiconductor wire inclusions placed between two metallic planes. The semiconductor wire inclusions had two values of conductivity σ: 10^4 S/m [(a) and (c)] and 10^2 S/m [(b) and (d)]. The calculations were made for $H_0 = 795.8$ A/m, $M_0 = 0.014$ T, $\varepsilon_r = 16$, $r_1 = 100$ μm, $r_2 = 300$ μm, $T = 2$ mm, $d = 0.5$ mm, and $\sigma = 10^8$ S/m.

orientation, when the wire conductivity corresponds to graphite. The BEMW is well observed at small wave-number values and attenuates at large wave numbers. For the germanium wires, the BEMW is not observed at all.

IV. CONCLUSION

By using the approximate analytical electrodynamic model of the transversally magnetized FM metamaterial layer with wire inclusions, we demonstrated that all slow (forward and backward) waves existing in such structure are the electromagnetic waves. For the slow FEMW, we established that the electrical energy predominates away from the FM

resonance frequency, and near this frequency the magnetic energy predominates. For the slow BEMW, the magnetic energy predominates away from the plasma frequency, and near this frequency the electrical energy predominates. By using the MaxLLG software, we showed that the BEMW can exist in both the infinite FM metamaterial and the FM metamaterial layer metallized on both sides. The BEMW control was realized by the change in the external uniform magnetic field orientation, the FM metamaterial thickness, the wire connection to the metallic plates, and the wire conductivity. We established that the BEMW disappears in the infinite FM metamaterial, when the bias field orientation is changed from transverse to longitudinal. The BEMW appears again in the magnetized FM metamaterial layer if the metallic plates are placed on both sides of the FM metamaterial layer and the wire inclusions are connected to the metallic plates. For the normal bias field orientation, the BEMW exists both in thick and in thin FM metamaterial layers. For the longitudinal bias field orientation, the BEMW is observed only in relatively thin layers when the thickness d and the period of wire array T approximately satisfy the following condition: $d/2 \cong T = \lambda_{B1}/2$. Besides, the BEMW is observed even when the material of wire inclusions is a semiconductor—graphite.

The obtained results are of fundamental and applied interest related to the creation of controlled 2D magnetic metamaterials (metasurfaces) with DNM properties not only in the microwave but also in the terahertz frequency ranges [14]. The control of the BEMW existing in such metamaterials can be achieved not only by a magnetic field but also by an electric field [22], which changes the conductivity of semiconductors. It opens up the possibility of creation of double control (by magnetic and electric fields) functional devices based on the antiferromagnetic metamaterials with semiconductor wire inclusions for the terahertz range.

[1] V. G. Veselago, Electrodynamics of substances with simultaneously negative values ε and μ, Sov. Phys. Usp. **10**, 509 (1968).

[2] J. B. Pendry, A. J. Holden, W. J. Stewart, and I. Youngs, Extremely low frequency plasmons in metallic mesostructures, Phys. Rev. Lett. **76**, 4773 (1996).

[3] D. R. Smith, W. J. Padilla, D. C. Vier, S. C. Nemat-Nasser, and S. Schultz, Composite medium with simultaneously negative permeability and permittivity, Phys. Rev. Lett. **84**, 4184 (2000).

[4] J. B. Pendry, Negative refraction makes a perfect lens, Phys. Rev. Lett. **85**, 3966 (2000).

[5] Y. I. Bespyatykh, A. S. Bugaev, and I. E. Dikshtein, Surface polaritons in composite media with time dispersion of permittivity and permeability, Phys. Solid State **43**, 2130 (2001).

[6] A. V. Vashkovskii and E. Lokk, Negative refractive index for a surface magnetostatic wave propagating through the boundary between a ferrite and ferrite-insulator-metal media, Phys. Usp. **47**, 601 (2004).

[7] G. Dewar, Minimization of losses in a structure having a negative index of refraction, New J. Phys. **7**, 161 (2005).

[8] Y. He, P. He, S. D. Yoon, P. V. Parimic, F. J. Rachford, V. G. Harris, and C. Vittoria, Tunable negative index metamaterial using yttrium iron garnet, J. Magn. Magn. Mater. **313**, 187 (2007).

[9] H. Zhao, J. Zhou, Q. Zhao, B. Li, L. Kang, and Y. Bai, Magnetotunable left-handed material consisting of yttrium iron garnet slab and metallic wires, Appl. Phys. Lett. **91**, 131107 (2007).

[10] K. Bi, J. Zhou, H. Zhao, X. Liu, and C. Lan, Tunable dual-band negative refractive index in ferrite-based metamaterials, Opt. Express **21**, 10746 (2013).

[11] F. J. Rachford, D. N. Armstead, V. G. Harris, and C. Vittoria, Simulations of ferrite-dielectric-wire composite negative index materials, Phys. Rev. Lett. **99**, 057202 (2007).

[12] A. G. Gurevich and G. A. Melkov, *Magnetization Oscillations and Waves* (CRC Press, Boca Raton, FL, 1996).

[13] Y. J. Huang, G. J. Wen, T. Q. Li, J. L. W. Li, and K. Xie, Design and characterization of tunable terahertz metamaterials with broad bandwidth and low loss, IEEE AWP Lett. **11**, 264 (2012).

[14] S. V. Grishin, M. D. Amel'chenko, Y. P. Sharaevskii, and S. A. Nikitov, Double negative media based on antiferromagnetic metamaterials, Tech. Phys. Lett. **48**, 18 (2022).

[15] M. D. Amel'chenko, S. V. Grishin, and Y. P. Sharaevskii, Fast and slow electromagnetic waves in a longitudinally magnetized thin-film ferromagnetic metamaterial, Tech. Phys. Lett. **45**, 1182 (2019).

[16] High Frequency Magnetics Software (2019) [https://www.maxllg.com].

[17] A. L. Mikaelyan, *Theory and Practice of Microwave Ferrites* (State Power Press, Moscow, 1963).

[18] L. D. Landau and E. M. Lifshitz, *Course of Theoretical Physic, Physical Kinetics,* Vol. 10 (Pergamon Press, Oxford, 1981).

[19] M. M. Aziz, Sub-nanosecond electromagnetic-micromagnetic dynamic simulations using the finite-difference time-domain method, PIER B **15**, 1 (2009).

[20] See Supplemental Material at http://link.aps.org/supplemental/10.1103/PhysRevB.108.224401 for the description of the numerical simulation process conducted using MaxLLG software, which includes Refs. [7,19,21].

[21] A. Taflove and S. C. Hagness, *Computational Electrodynamics: The Finite-difference Time-domain Method* (Arctech House, Boston, MA, 2000).

[22] M. A. Morozova, D. V. Romanenko, A. A. Serdobintsev, O. V. Matveev, Y. P. Sharaevskii, and S. A. Nikitov, Magnonic crystal-semiconductor heterostructure: Double electric and magnetic fields control of spin waves properties, J. Magn. Magn. Mater. **514**, 167202 (2020).